Electrical, thermal and mechanical properties of poly-etherimide epoxy-diamine blend

Nour Halawani, Jean-Louis Augé, Hervé Morel, O. Gain, S. Pruvost

Composites Part B 110 (2017) 530–541

Contents lists available at ScienceDirect

Composites Part B

journal homepage: www.elsevier.com/locate/compositesb

Electrical, thermal and mechanical properties of poly-etherimide epoxy-diamine blend

N. Halawani [a, b], J.L. Augé [a], H. Morel [a], O. Gain [b], S. Pruvost [b, *]

[a] Univ Lyon, INSA Lyon, UMR CNRS 5005, AMPERE, F- 69622, Villeurbanne, France
[b] Univ Lyon, INSA Lyon, UMR CNRS 5223, IMP Ingénierie des Matériaux Polymères, F-69621, Villeurbanne, France

ARTICLE INFO

Article history:
Received 11 August 2016
Received in revised form
6 October 2016
Accepted 11 November 2016
Available online 12 November 2016

Keywords:
Thermosetting resin
Organic-organic blend
Thermoplastic
Electrical properties

ABSTRACT

This work deals with the study of thermoset-thermoplastic blend forming an epoxy-amine/poly-etherimide phase separated to assess the dielectric and thermal performances. These materials would be good candidates to replace the passivation layer in semiconductors, particularly ones used as switches in power electronic applications. Polyimide and Parylene are usually quoted and studied. Mixtures based on polymers would be a novel candidate that can manage to be an insulator for the system. The modified and non-modified systems where characterized by transmission electron microscopy, scanning electron microscopy, differential scanning calorimetry, thermogravimetric analysis, dynamic mechanical analysis, dielectric analysis and analytical simulation was carried out on dielectric measurements. These complementary techniques were used first to investigate the presence of the phase separation phenomenon and second to quantify the separated nodules size. The effect of this phase separation was examined and showed enhancement in the dielectric values compared to the pure epoxy system. It was finally simulated to show a close assumption of what is found experimentally.

1. Introduction

In power IGBT (insulated-gate bipolar transistor) modules, the organic insulating materials as polyimide and silicone are mainly present. Polyimide is deposited by spin coating while silicone gel is deposited by molding under vacuum. These materials play a significant role in the improvement of the package voltage ratings under high tension and even if the temperature range for using silicone is limited for around 200 °C under a continuous use. On the other side, the softness and high electrical properties of silicones render it interesting. Furthermore, under high voltage partial discharge can give rise to the breakdown of the device. In an alternator, the reduction of the partial discharges effect was carried out by incorporating mica flakes in the insulating material to play the role of a barrier against discharges [1]. The goal of this paper is to present a novel material that could be another good candidate used as passivation layer or the encapsulation layer in the power modules.

Generally, composites are made up of materials combinations differing in composition, where the individual constituents retain their separate identities. Separate constituents acting together give the final morphology and property of the composite.

Polymers composites are one of the most famous composites, such as metal matrix composites (MMC) or ceramic matrix composites (CMC), commercially used and studied in several domains such as electrical engineering due to their good dielectric properties, light weight and ease of production [2–8]. One of the studied kinds of polymer composites is epoxy filled with inorganic micro or nano particles; it is an organic-inorganic blend. Epoxy networks are extensively used as highly crosslinked materials in many applications due to their special performance, such as good mechanical, thermal and electrical properties as well as low thermal expansion coefficient compared to silicon gels. They are now widely used in many applications such as adhesives, coatings, construction, and composite matrices in the aerospace and electronics industries. Many investigations are done to show and compare the effects of nano and micro fillers on the final electrical characteristics of the epoxy network [9–14]. With the addition of micro-fillers to the epoxy network, the relative permittivity of the epoxy micro-composite is always higher than that of the pure epoxy network [11,12]. Nanocomposites with relatively low filler concentrations, i.e., less than 1 vol%, pointed out a relative permittivity ε'_r which is lower than that of both the neat epoxy network and the filler but

* Corresponding author.
E-mail address: sebastien.pruvost@insa-lyon.fr (S. Pruvost).

http://dx.doi.org/10.1016/j.compositesb.2016.11.022
1359-8368/

with an increase in the loss values [14–16]. They also presented improvements in both thermal and electrical properties [14,17–19]. As the filler concentration increases, the real permittivity of nanocomposites can be much higher than the pure epoxy network. Behavior of the nanocomposites depends on both the permittivity and the concentration of the fillers.

Another kind of polymer blend is the mixture of polymer with another organic substituent, organic-organic blend wherein this mixture can produce miscible or immiscible systems. Immiscible block copolymers are widely studied in a way many parameters can be adjusted and other organic structures can be added in order to change the miscibility of the mixture [20–22]. Nonetheless, miscible mixtures of polymer and organic mixtures such as thermoplastic-thermoset blends have gained importance in the previous decades. Adding a thermoplastic to the thermoset network (with phase separation) can improve some of the mechanical properties of the thermoset, such as network resistance toughness [23]. In most cases the thermoplastic-thermoset blends are prepared starting from a homogenous solution of the thermoplastic polymer in the prepolymer and during the polymerization of the thermoset a phase separation occurs in the blend at a given epoxy conversion rate. This mechanism is known as reaction-induced phase separation [24,25] and may lead to several morphological types such as particulate, bicontinuous, or phase inverted, an illustration schema is presented in Fig. 1 The separation proceeds via the spinodal demixing (SD) mechanism and thus the obtained system is homogenous. Many attempts have been made to modify epoxy networks with high performance engineering thermoplastics that are characterized by high Tg and high toughness, such as polysulphone (PSF) [26,27], Poly-ethersulfone (PES) [28–30] and poly-etherimides (PEI) [23,31–36]. Commercial products exhibit large variation in average molar masses of engineering thermoplastics and thus provide different modification to the epoxy properties [24].

Investigation of phase separation behavior in PEI-modified epoxy networks was done extensively since 1989 [31]. Tetrafunctional epoxy resins tetraglycidyl 4,4′-diaminodiphenylmethane (DGDDM) was blended with PEI toughening agents and using 4,4′-diaminodiphenylsulfone (DDS) as curing agent [37]. SEM micrographs reveal spherical PEI domains in epoxy network at 5 wt% PEI used and these domains became larger as the PEI contents were increased up to 20 wt%. Bonnet et al. worked on Bisphenol A diglycidyl ether (DGEBA) prepolymer with PEI and confirmed these observations associated to an improvement in the fracture toughness of the blend at room temperature due to the presence of PEI [23,36]. The improvement increases along with the increase of the PEI percentage blended with the epoxy network [38].

This study deals with the effect of phase separation phenomenon in an organic-organic blend on the thermal, mechanical and electrical properties. The chosen thermoset matrix is an epoxy-amine network in which PEI is added to obtain the phase separation with nodules of PEI inside the thermoset matrix. The chosen epoxy system is a model system with controlled reactivity [39]. To insure the stability of the epoxy system along a wide range of temperature, the epoxy system chosen have high glass transition Temperature (T_g) of around 160 °C, and the thermoplastic, PEI, have higher T_g around 220 °C.

2. Experimental

2.1. Materials

The epoxy prepolymer used was Diglycidyl ether of bisphenol A, liquid at room temperature, $DGEBA_{\overline{n}=0.15}$ (Araldite LY556 from Huntsman). The curing agent was an aromatic diamine, 4,4'-methylenebis-[2,6-diethylaniline], M-DEA supplied by Lonzacure™. The diamine was added in the stoichiometric ratio, epoxy to amine hydrogen groups equal to 1, in pure and modified mixtures. The thermoplastic used was Polyetherimide, PEI Ultem 1010, supplied by General electric. The chemical structures are listed below in Table 1.

To prepare the neat network (without thermoplastic), the diamine was added to the epoxy prepolymer heated at 90 °C and stirred under vacuum. The PEI modified mixture was prepared in a three-step process: first PEI was heated at 150 °C for several hours to remove possible humidity in the powder, then dissolved in the epoxy prepolymer at 140 °C, and finally the diamine was added at 90 °C. The two mixtures were stirred under vacuum and poured in silicon preheated molds. For insuring a complete crosslinking process, the curing process was 4 h at 135 °C followed by 2 h at 200 °C of post-curing for pure epoxy network and 4 h at 160 °C followed by 2 h at 185 °C of post-curing for PEI modified mixture. Then the mixtures were left to cool down to room temperature. Precuring durations where chosen larger than the vitrification time to be sure that most of the microstructures are developed isothermally. The precuring temperature determines the final morphology of the PEI thermoplastic into the epoxy network [23,40]. PEI pure films were prepared by pressing PEI powder at 270 °C under 30 bars. The obtained film has a thickness of 0.2 mm.

For the designation of the systems, the term DM corresponds to the epoxy-amine (DGEBA-MDEA) system without thermoplastic, which is also called neat network, and DM10PEI denotes the system DGEBA-MDEA modified with 10 wt% of PEI.

2.2. Techniques

Phase separation as well as size distribution of the PEI nodules in the epoxy network was observed by Scanning Electron Microscopy (SEM) Microscope ESEM-FEG FEI XL30 at CLYM (Centre LYonnais des Microscopies) using secondary electrons. Fractured Samples were etched with a 1 wt% solution of potassium permanganate in a 5:2:2 vol mixture of concentrated sulfuric acid-

Fig. 1. Scheme presenting different morphological type of phase separation; left to right: particulate, bi-continuous and phase inverted.

Table 1
Chemical structures of the used reactants.

Reactants	Formula	Supplier	$\overline{M_n}$(g.mol^{-1})
DGEBA	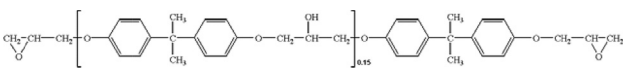	Huntsman	382
MDEA	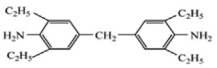	LONZA	310
PEI	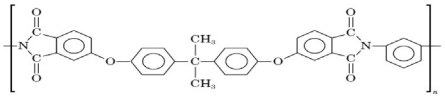	GE	26,000

phosphoric acid-distilled water. After etching, the samples were sequentially washed in aqueous sulfuric acid, hydrogen peroxide (100 vol), water, and finally acetone [41]. All samples were then sputter coated with gold before SEM examination. Size distribution of the dispersed nodules was obtained using ImageJ software.

TEM analysis was performed on Philips CM120 transmission electron microscope (at the Centre Technologique des Microstructures CTμ of the University of Lyon) with an accelerating voltage of 80 kV. Epoxy samples were trimmed using an ultra-microtome and the slices (60–70 nm in thickness) were placed onto 300 mesh copper grids for observation.

Glass transition temperature, determined as midpoint temperature T_g, midpoint, of the epoxy-amine systems was measured using Differential Scanning Calorimetry (DSC) TA Q20. Experiments were carried out on a 5 mg sample under controlled atmosphere of helium in a temperature range from −100 to 300 °C at a heating rate of 10 °C/min. Temperature and heat flow were calibrated using indium.

The thermogravimetric analysis (TGA) were performed using TA Q500 analyzer from 25 °C to 800 °C at a heating rate of 10 °C/min in both air and nitrogen atmospheres.

Dynamic mechanical analysis (DMA) was carried out using a TA Q800 instrument with a heating rate of 3 °C/min. Tensile testing clamp for rectangular samples was used. Samples tested are of a rectangular shape with a thickness between 0.5 and 1 mm, a length of 20 mm and a width of 10 mm. The tensile strain is applied at a frequency of 1 Hz and its value is equal to 0.01%. Storage modulus E′, Loss Modulus E″ and the loss factor tan δ were measured during temperature ramps from −100 °C up to 300 °C with a rate of 3 °C/min.

Solatron analytical (Modulab MTS) dielectric spectrometer, equipped with the LakeShore 335 Temperature controller, is used to characterize the dielectric properties of samples under a temperature range of −100 to 250 °C in a Helium atmosphere. Temperature control is guided by the use of liquid nitrogen circulating around the chamber that contains the sample. Measuring is done after heating steps of 3 °C under the frequency of 10^6 to 10^{-1} Hz and Vrms = 5 V. Samples used are of circular shape with a 3 cm diameter and a thickness between 0.5 and 1 mm. Two gold electrodes, of 25 mm in diameter, were sputtered on both sides using BAL-TEC SCD 005 Cool Sputter Coater. The model used for measurement is metal-insulator-metal (MIM) capacitor.

3. Results and discussion

3.1. Morphology of cured epoxy-PEI blend

SEM images were performed on the neat network and 10 wt% PEI in the epoxy-amine network and shown in Fig. 2(a) and (b) respectively. The aim was to observe if the phase separation phenomenon occurs between PEI and the epoxy network. The dark part corresponds to the epoxy rich phase and the bright parts correspond to the PEI rich phase. It can be seen that the phase separation produced a well dispersed PEI phase in a continuous epoxy network. Due to the low reactivity of the DGEBA-MDEA system, the separation proceeded via the spinodal demixing (SD) mechanism [32].

The size distribution of the nodules inside the epoxy-amine network is presented in Fig. 2(b) The separated nodules have a spherical or ellipsoidal form with an average diameter between 2 and 3 μm. From literature [31,33,34], a similar morphology was observed for the same range of weight percentage of PEI but within a tetrafunctional amine hardener. Temperature of precuring affects the nature of the reactions in an epoxy-amine/thermoplastic mixture and governs the structure/morphology of the resultant blends. It has been shown that slower epoxy curing rate and specifically precuring ones, where long gel times were obtained, resulted in non-spherical thermoplastic domains [23].

Fig. 3 shows a TEM image of the DM10PEI sample in which the phase separation phenomenon observed by means of SEM. The dark part corresponds to the PEI phase and the bright part corresponds to the epoxy phase. An interphase is seen surrounding the PEI separated nodules having a thickness of 20–50 nm. This interphase is not found to be present surrounding all the nodules.

3.2. Thermal properties

Thermogravimetric diagrams under air and nitrogen atmosphere of the three systems are displayed in Fig. 4 (a) and (b) respectively. The system is considered stable until 5% of its mass is lost. The neat epoxy system showed good thermal stability up to 300 °C under air atmosphere and up to 350 °C under nitrogen atmosphere with a T_{max} peak of the derivative weight change at 380 °C and 400 °C respectively. Afterwards, chain scission of the network takes place yielding combustible gases, water, amines, and gaseous aromatic compounds, etc. [42]. The lower temperature degradation observed under air can be explained by the presence of the oxidation phenomenon. The pure PEI system showed similar stability under both atmospheres up to 525 °C with a difference in the residual mass. The addition of PEI in the epoxy network did not significantly affect its thermal stability upon modifying it with 10 wt% of PEI.

3.3. Glass transition temperature

Fig. 5 (a) shows DSC measurements realized on the three studied systems (Epoxy network, Epoxy-PEI network and PEI). PEI film showed a transition corresponding to the glass transition at

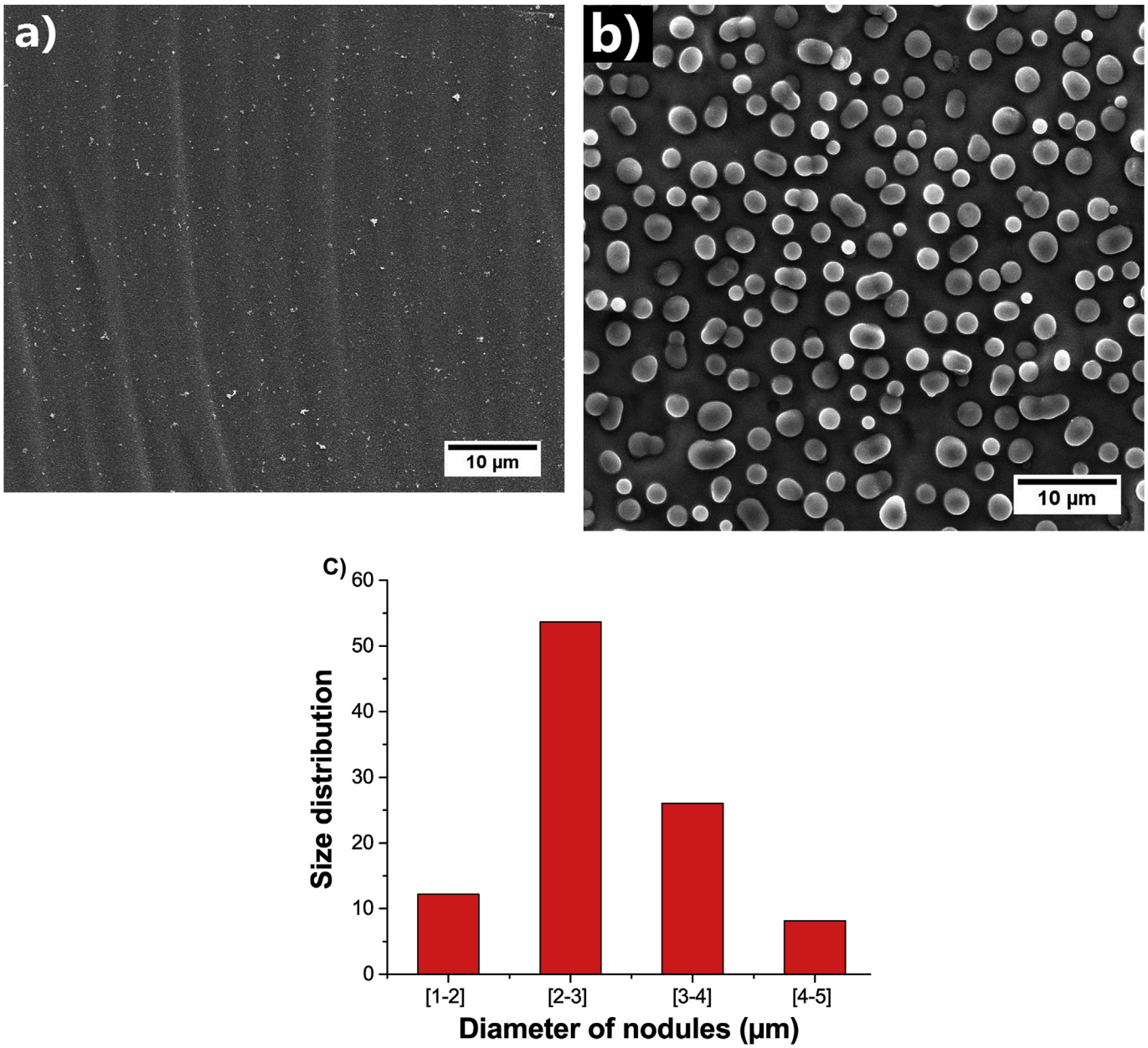

Fig. 2. SEM image of DM (a) DM10PEI blend (b) and Size distribution of the PEI nodules into the epoxy network (c).

216 °C. DM sample showed also a single transition corresponding to the glass transition temperature of epoxy-amine network at 164 °C. The DM10PEI sample exhibited a transition similar to the latter with the same value of specific heat constant having values of 0.15 J/(g.°C). Both DM and DM10PEI did not present an exothermic peak on the first run, which insures full cross-linking of the epoxy amine network. The same temperature of the glass transition obtained on the second run (increasing temperature) confirmed this result. The glass transition corresponding to the thermoplastic phase in the epoxy network is not marked due to its low concentration in the system. A derivative of the heat flow of the DM10PEI system with respect to temperature is shown in Fig. 5(b) where the second transition of the system can be observed at 216 °C corresponding to the glass transition temperature of the PEI. Phase separation phenomenon is confirmed by the presence of two glass transitions in the DM10PEI system corresponding to the two separated systems Epoxy-MDEA and PEI. Both the transition of the epoxy and the PEI systems were not shifted upon the presence in the DM10PEI network which proved a total phase separation of the system.

Dynamic mechanical data are plotted in Fig. 6 for DM, DM10PEI and PEI. The storage moduli curves are depicted in Fig. 6(a); DM showed a constant stable value over a wide range of temperature and up to α relaxation temperature (T_α epoxy = 183 °C) of the epoxy network where the decay of the storage modulus was observed. The storage modulus value is higher for PEI than for DM. At 226 °C, the relaxation α associated to the glass transition of PEI T_α (PEI) appeared. The 10 wt% PEI/epoxy blend followed the same evolution as that of the neat system with the same decay phenomenon corresponding to T_α (epoxy).

Tan delta curves in Fig. 6(b) underline that the neat epoxy network gives two loss peaks. One broad peak at low temperature with a maximum at −60 °C was assigned to the β relaxation (T_β)

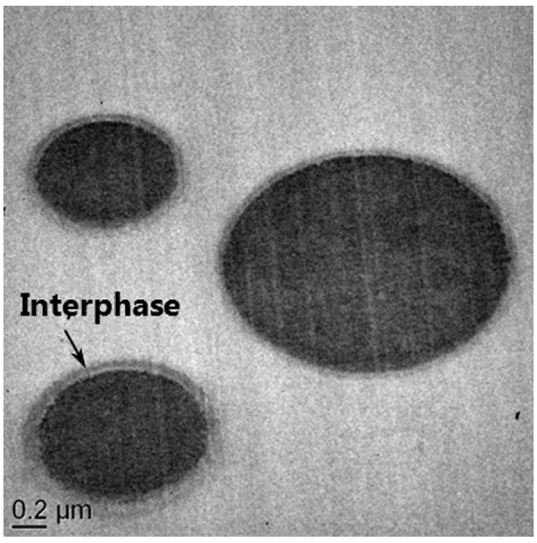

Fig. 3. TEM image of DM10PEI.

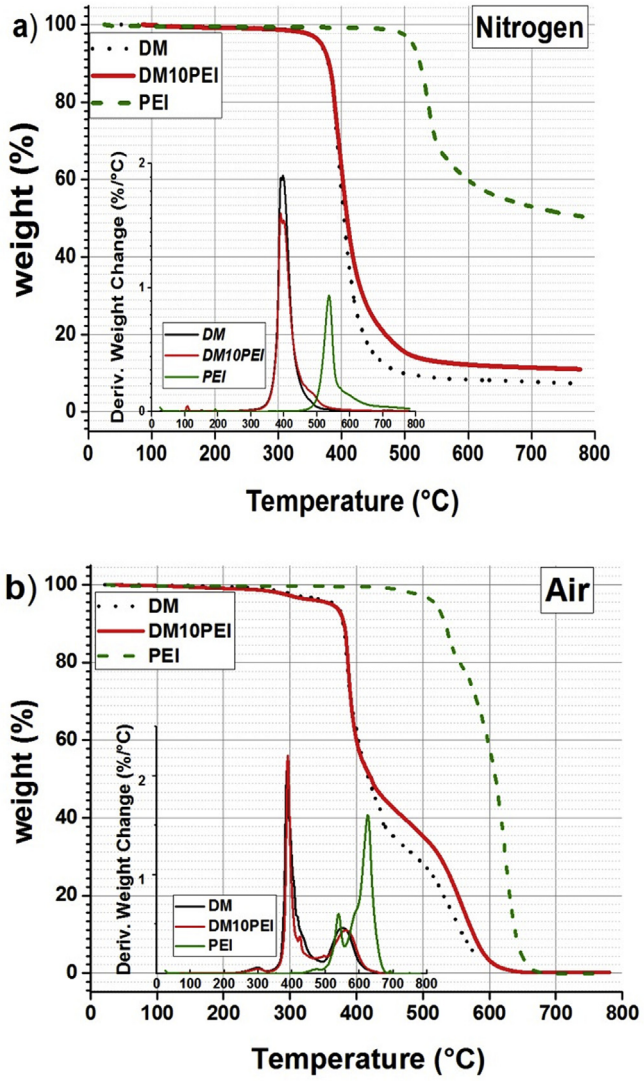

Fig. 4. Weight loss as a function of temperature for DM, DM10PEI and PEI a) in nitrogen atmosphere; b) in air atmosphere.

attributed to the movement of the hydroxyether units (—O—CH_2—CH(OH)—CH_2—) created by the crosslinking reaction and the initial epoxy prepolymer [43]. A second sharp peak corresponding to T_α associated to the glass transition temperature of epoxy network is observed at 183 °C. The α relaxation in epoxy networks depends on the nature of the epoxy prepolymer as well as the hardener [12,29,41–44]. One sharp peak with a maximum at 229 °C is observed and ascribed to T_α associated to the glass transition of PEI.

The phase separation phenomenon, suggested by SEM images, for the 10 wt% PEI/epoxy blend (so-called DM10PEI) is confirmed in the DMA measurements by the presence of two high-temperature relaxations associated to the epoxy network ($T_{\alpha 1}$) and the PEI phase ($T_{\alpha 2}$) respectively. DM and DM10PEI exhibited the same temperature for α relaxation of the epoxy network proving that the epoxy network is totally separated from the thermoplastic. Alternatively, $T_{\alpha 2}$ is slightly lower than pure PEI by 6 °C. This shift could be attributed to two different phenomena. First, a small amount of epoxy-amine is miscible in the PEI phase plasticizing it. Secondly, the presence of free volume, in which it has been shown that blending of polymers generate additional free volume, which can lower Tg by reducing the energy necessary for segmental motion [23,45]. In the next part, these two possibilities will be discussed.

In addition to SEM images, more information about the morphology of the system can be obtained by studying the heights of loss peaks and, more specifically, the ratio of these heights (h_2/h_1). This value appears to be very sensitive not only to the volume fraction but also to the shape of final morphology through the choice of the curing temperature. The characteristics of the two high temperature loss peaks, their maximum temperature ($T_{\alpha 1}$, $T_{\alpha 2}$), their amplitudes (h_1, h_2), the ratio of these heights (h_2/h_1) as well as the values of the storage modulus before and after the α relaxation temperature are collected in Table 2. The amplitude of the peak corresponding to the epoxy network (h_1) remains constant with the addition of PEI. On the other hand, the amplitude of the peak corresponding to the PEI into the epoxy network is significantly reduced due to the low percentage of PEI present in the epoxy network [38].

The ratio (h_2/h_1) can be used to predict qualitatively the kind of morphology generated in thermoplastic/thermoset blends and to know if the structure of the network is inverted or not. In this studied case of DM10PEI, its ratio is equal to 0.14. This value corresponds to the morphology of the separated nodules in the epoxy network as described by Girard-Reydet et al. [23] and confirms the particulate morphology observed by SEM. The particulate morphology of PEI into the epoxy network did not affect the value of storage modulus of the epoxy network. Nevertheless it have been noted that the PEI nodules formed an obstacle to the propagation of mechanical crack and may participate to the crack blunting effect [23].

3.4. Dielectric properties

Dielectric measurements were carried out on the three systems to monitor the influence of the addition of the thermoplastic material into the epoxy network; their dielectric response is presented in Fig. 7(a). The real (ε'_r) and the imaginary (ε''_r) parts of the dielectric relative permittivity were derived from measurements under a 3 V_{rms} sinusoidal applied voltage.

Regarding the dielectric response at a constant frequency of 1 kHz versus temperature Fig. 7(a), the neat epoxy network showed relative permittivity ε'_r values starting from 4.5 at low temperatures and increasing up to 6.5 at temperatures higher than ambient temperature. A small increase with a maximum value around 183 °C corresponds to the α relaxation of the epoxy system. PEI has

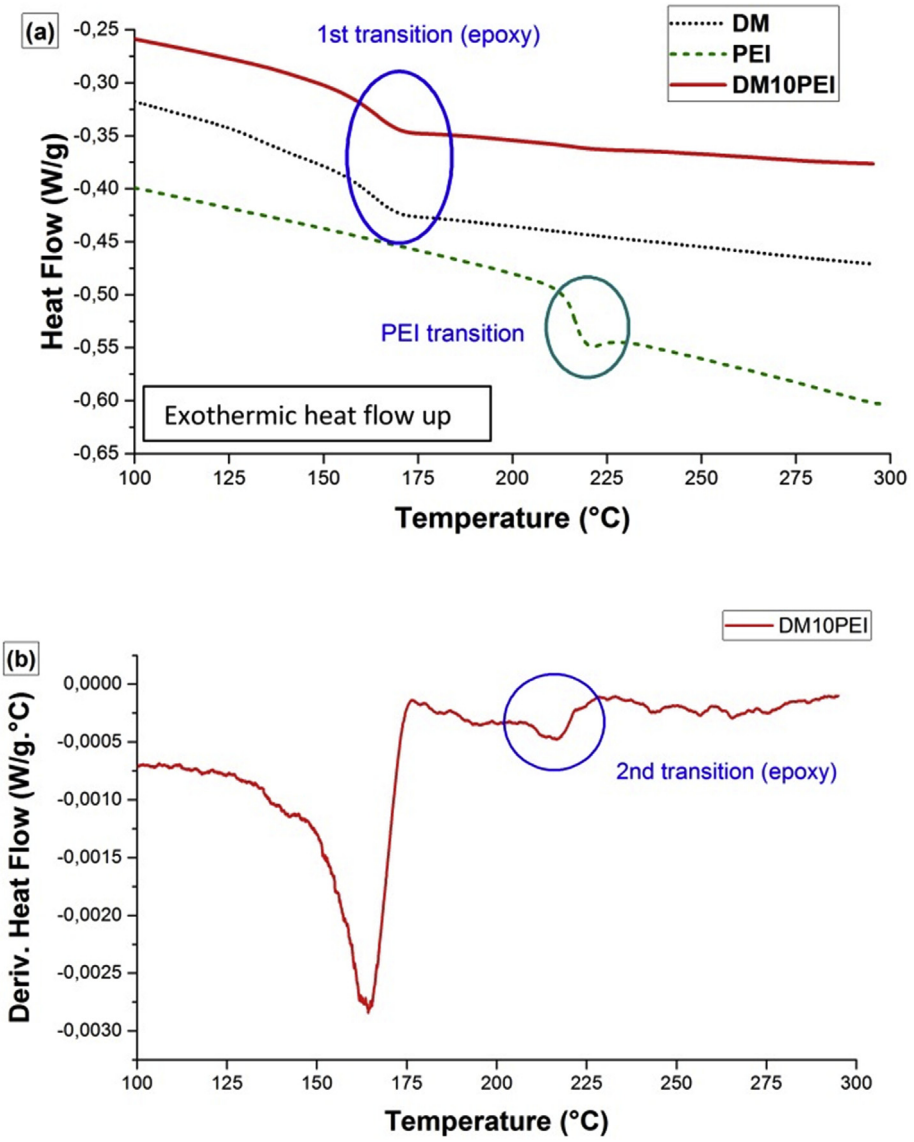

Fig. 5. DSC thermograms of DM, DM10PEI and PEI and b) Derivative of heat flow with respect to temperature of DM10PEI.

relative permittivity ε'_r values lower by 30% than that of the neat epoxy network and constant on the whole range of temperatures. Choudhury et al. observed similar results for the relative permittivity ε'_r of PEI [46]. The introduction of 10 wt% of PEI into the epoxy network led to a decrease of around 15% of the relative real permittivity ε'_r. The shape of the curves was not influenced by the addition of PEI but it was only shifted to lower values.

Imaginary relative permittivity values ε''_r Fig. 7(b) of epoxy network two main transitions are identified. The first transition at −30 °C corresponds to β transition associated to the movement of the hydroxyether units created by the crosslinking reaction and the initial epoxy prepolymer. The second main transition starting at 170 °C corresponds to α transition of epoxy network that appears in the form of a shoulder superimposed on the conduction phenomenon; this transition was also observed in DMA measurements. PEI network exhibited one main α relaxation at 240 °C associated to the glass transition of PEI. The introduction of 10%wt of PEI into the epoxy network lowered the relative imaginary permittivity by 15% from −100 °C to 200 °C. The system showed the presence of both α and β relaxations corresponding to epoxy network. α transition corresponding to the PEI inclusion is not fully recognized due to the limitation of the experimental temperature at 230 °C.

Loss values tested in all frequency and temperature ranges are represented in a 3D plot Fig. 8(b). The value of the losses ε''_r decreased slightly below Tα epoxy upon the addition of PEI. First relaxation whose maximum is around −50 °C is supposed to be the β relaxation of the epoxy network, where it is shifted with the variation of frequency. When the temperature approaches the glass transition temperature of the epoxy system a huge increase in the loss values is identified. The beginning of this increase is due to α relaxation of the epoxy network, related to relaxation processes of the main chains of the cross-linked epoxy chains, where it is partially mask due to the increase of the concentration of charge carriers. This relaxation arises from the fact that free charges are now immobilized in the material, and at sufficient high temperature, the charges can migrate in the presence of applied electric fields. As the temperature increase above the glass transition temperature, the conductivity of the system increases giving rise the increase of the concentration of charge carriers. This increase is seen in DM as well as DM10PEI. This increase is relatively higher in

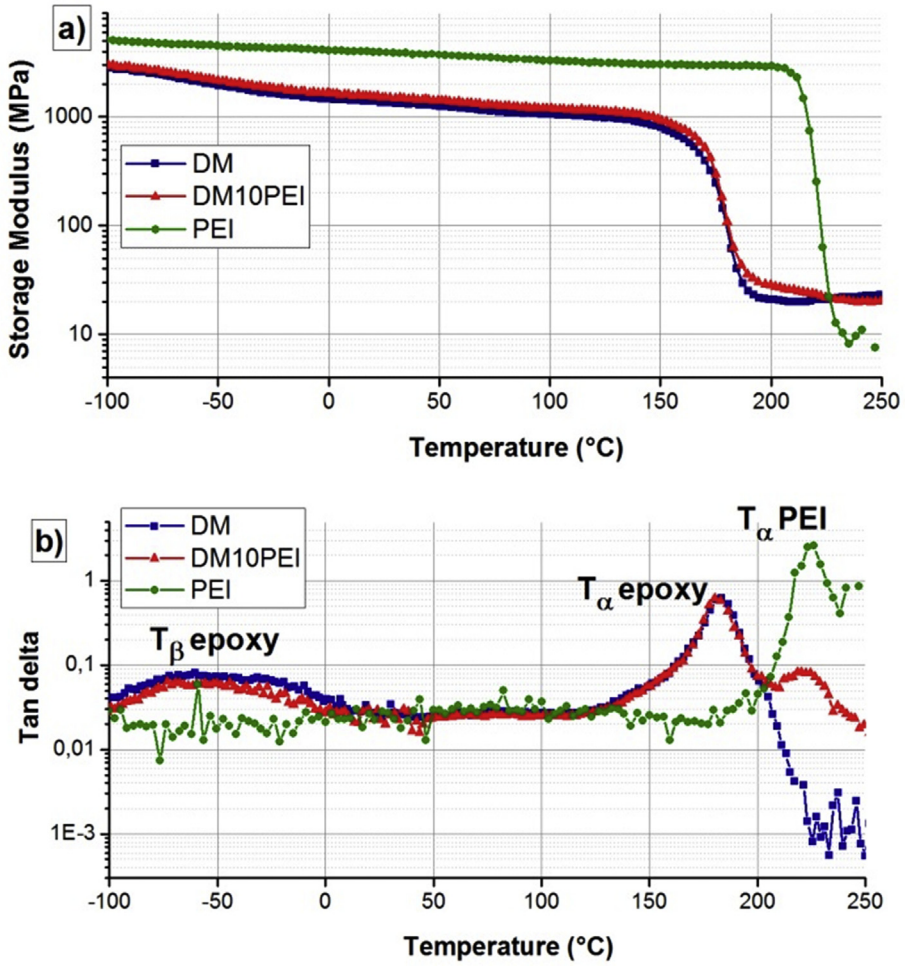

Fig. 6. Storage Modulus E' (a) and loss factor Tan δ (b) as function of temperature of DM, DM10PEI and PEI at 1 Hz.

Table 2
Temperatures ($T_{\alpha 1}$, $T_{\alpha 2}$), amplitudes (h_1, h_2) obtained from Tan δ curves Fig. 5(b), and storage modulus for DM, DM10PEI and PEI.

	T_α (°C)		Amplitude (h)		h_2/h_1
	$T_{\alpha 1}$	$T_{\alpha 2}$	h_1	h_2	
DM	183		0.62		–
DM10PEI	183	220	0.57	0.08	0.14
PEI	226		2.58		–

the 10 wt% PEI/epoxy blend where Maxwell-Wagner-Sillars (MWS) polarization can interfere as the process of (MWS) polarization exist in heterogeneous dielectrics, and is due to a delay in charge transfer at the interface between components with different dielectric permittivity [13].

Regarding other studies of micro and nano filled epoxy networks, dielectric properties is studied for systems filled with inorganic fillers, which is substantially different with the present system were the epoxy is blended with an organic PEI thermoplastic. It is noticed that the majority of the fillers have permittivity higher than that of the epoxy networks. According to literature, when micro-fillers are added to the epoxy network, the permittivity of the final epoxy micro-composite is higher than that of the pure epoxy network [11,12,47,48]. It's noteworthy that the incorporation of small percentages of nano-fillers (<2.5 vol%) in the presence of micro-fillers decrease the value of the epoxy micro-composite; however the real relative permittivity value as well as its imaginary relative permittivity still have higher values than the pure epoxy system [11,12].

The only way to decrease the permittivity value of the epoxy composite below the pure epoxy system was to add nano-fillers with small critical values depending on their nature [11,15,16,47–49]. These studies showed that the real and imaginary parts of the relative permittivity of the epoxy nano-composite have increased under the influence of nano-fillers above a small critical value, such as 0.5–1 vol% of hexagonal boron nitride (hBN), TiO_2, Al_2O_3 and ZnO [14,49], 2.5 vol % of barium titanate (BTO), calcium copper titanate (CCTO) and nano-silica [11,16], 5 vol % fumed silica and cubic boron nitride (cBN) [15,47]. Below these critical values the permittivity of the epoxy nano-composite decreases along with different responses in the loss factor. For example, the losses found to be stable using 20 nm nano-sized silica [11], higher for fumed silica, nano-sized BTO and CCTO, and 70 nm hBN [14–16] and relatively lower using 20–70 nm TiO_2, Al_2O_3, ZnO and cBN [47–49]. All the presented critical values were much smaller than the 9.8 vol % of organic PEI blended with the epoxy network used in our study. In comparison with the work of Fothergill et al. where they used 10 wt% of TiO_2 with an average size of 23 nm, the relative permittivity response was highly elevated due to the percolation phenomenon [50]. In the present study, the introduction of micro-fillers into the epoxy network leads to a decrease of the relative permittivity ε'_r without increasing losses, behavior in total

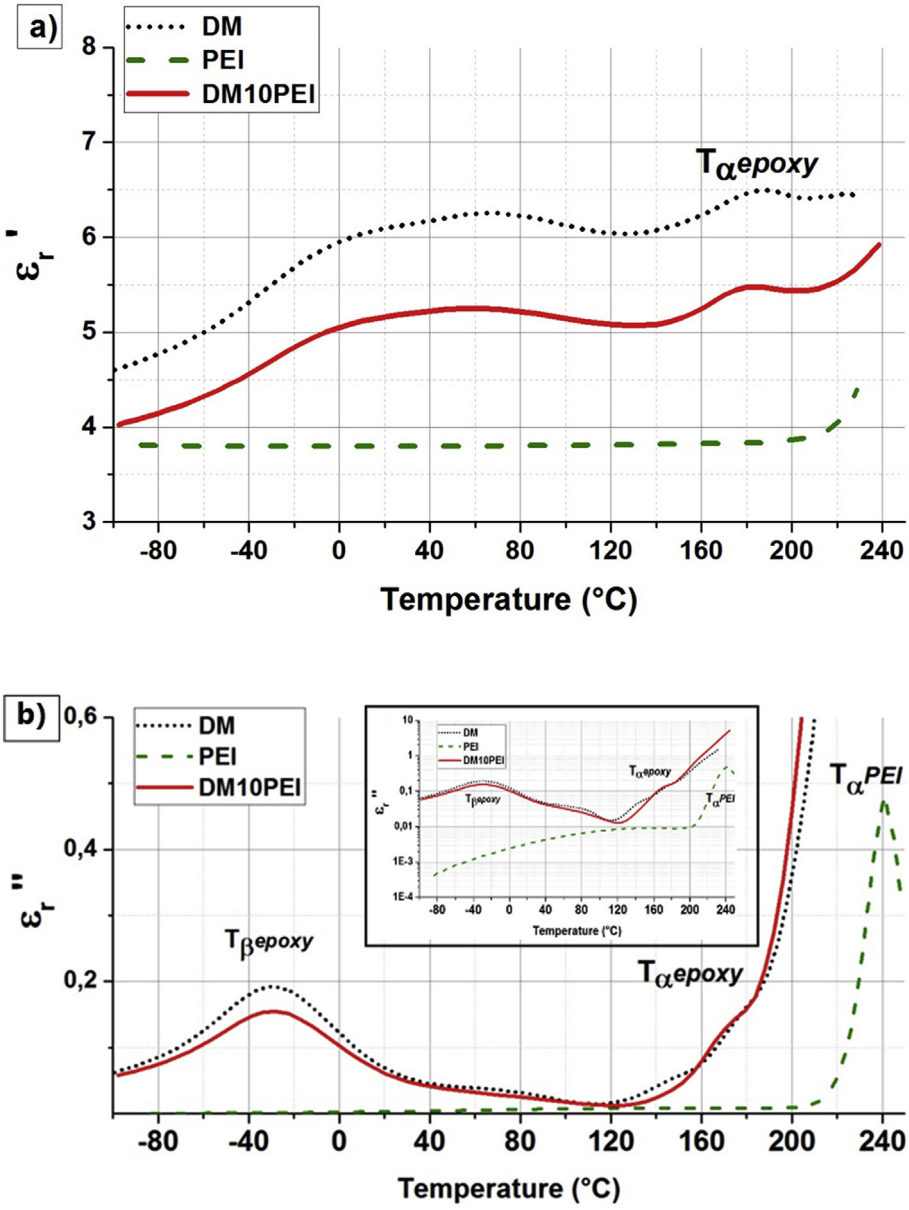

Fig. 7. Relative permittivity, b) Dielectric loss and zoom on the dielectric loss; as function of temperature at 1 kHz for DM, DM10PEI and PEI.

opposition to previous works on inorganic fillers. The presence of thermoplastic in the system proceeded in restricting the molecular dipolar movement of the epoxy system and thus decreases as well the relative permittivity response of the epoxy blend. We observed the decrease with the addition of PEI under all variations of temperature and frequency as seen in Fig. 8(a).

3.5. Effective permittivity

Simulation of the effective permittivity of the DM10PEI dielectric response was calculated from the experimental response of the pure systems of epoxy and PEI. The model, derived and studied by many authors [51–54], is an analytical formula of the global dielectric response of composite material consisting of a host matrix filled with ellipsoidal particles. The nodules are randomly oriented with respect to a given applied electric field as observed in the SEM image; Fig. 2(b). The effective permittivity of a medium having ellipsoidal inclusions can be expressed as

$$\varepsilon_e^* = \varepsilon_2^* \left(1 + \frac{1}{3} \varnothing \sum_{k=x,y,z} \frac{\varepsilon_1^* - \varepsilon_2^*}{\varepsilon_2^* + (\varepsilon_1^* - \varepsilon_2^*) L_k} \right) \quad (1)$$

where ε_e^*, ε_1^* and ε_2^* represent the calculated relative permittivity, experimental relative permittivity of PEI and the experimental relative permittivity of the epoxy network respectively. The real and imaginary parts of the complex relative permittivity are separated using computer software. A schematic representation of a PEI nodule in the epoxy network is shown in Fig. 9. The volume fraction $\varnothing = ((4/3)(\pi abc))/(lwh)$ of PEI in the epoxy network is, in our studied case, equal to 9.8 vol% where the densities of the DGEBA, MDEA and PEI are 1.15, 1.35 and 1.28 g/cm^3 respectively. L_k is the depolarization factor in the direction characterized by index k (x, y, z). A standard result of electrostatics gives [54]:

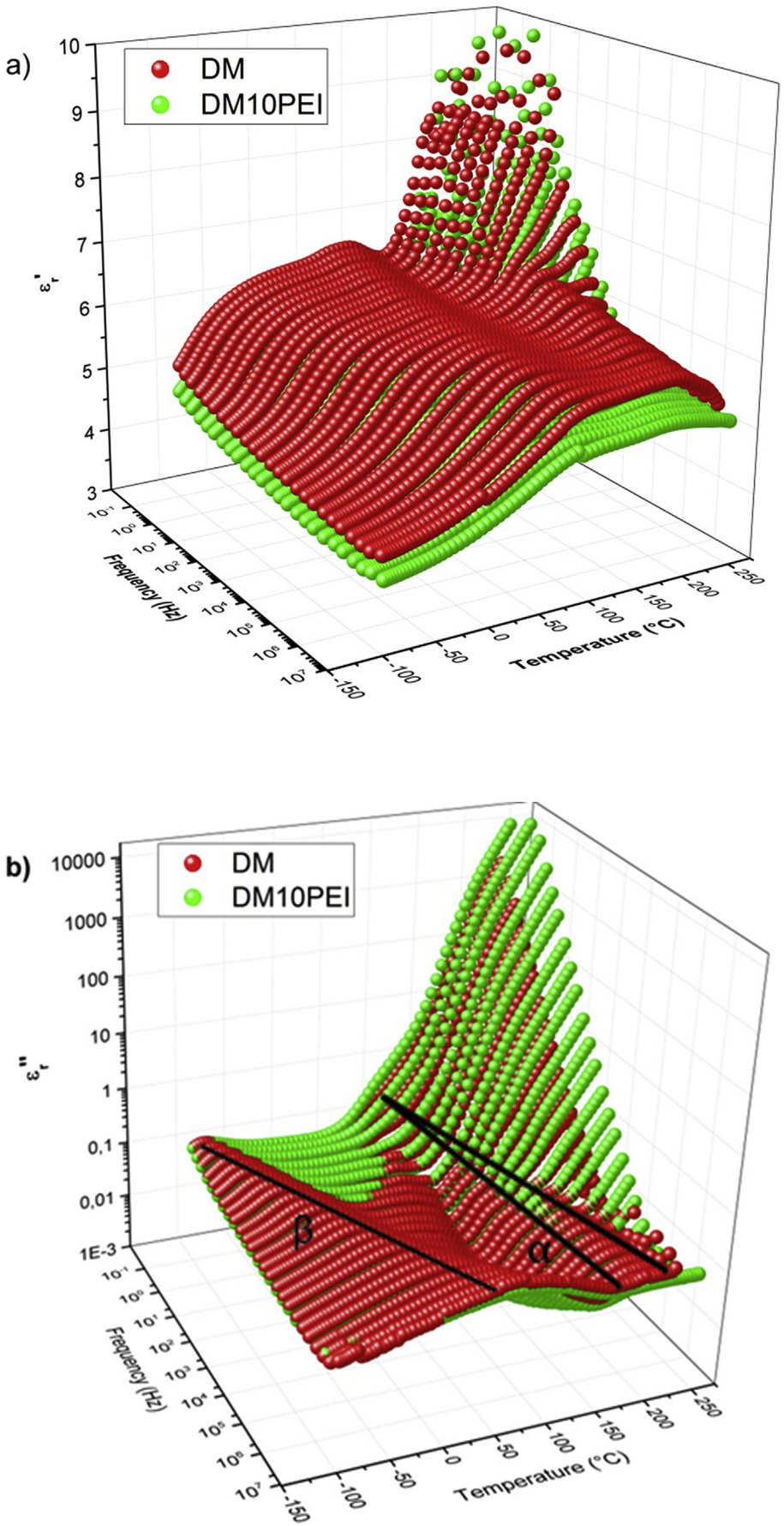

Fig. 8. Relative permittivity and b) Dielectric loss; of DM and DM10PEI versus temperature and frequency.

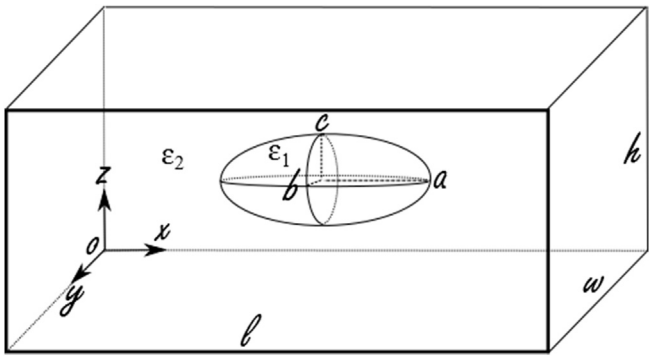

Fig. 9. Scheme of the PEI nodule into the epoxy network.

$$L_x = \frac{abc}{2}\int_0^{+\infty} \frac{du}{(u+a^2)\sqrt{(u+a^2)(u+b^2)(u+c^2)}} \quad (2)$$

Where a, b and c denote the semiaxes of the ellipsoid. As discussed earlier the average diameter of the PEI nodules into the epoxy network is 2–3 μm and thus the average major radius (a) is taken as 1–1.5 μm. The nodules are in an ellipse form having an average minor radius (b) = 4a/5 the major radius(a) and the second minor radius (c) is considered to be in the same size as (b); taking into consideration that the size of the particles is measured in 2D plane. For the studied epoxy-PEI blend, L is numerically calculated using (a) of value between 1 and 1.5 leading to a value of 0.275 and 0.362 for L_x and L_y respectively and Ly is equal to L_z.

SEM images showed that ellipsoidal nodules were regularly dispersed into the epoxy network. Furthermore, the system is considered to be randomly oriented with respect to the applied field. According to this fact, the summation of the three depolarization factors is applied in the proposed model. The simulated curve is calculated from the experimental permittivity of DM and PEI measured at 1 kHz and is presented in Fig. 10. The simulated curve is similar to the experimental one with a shift to higher values by an average of 9%. This shift can be explained in several points of view. From the theoretical work of Balberg et al. it can be suggested that excluded volume in PEI can be at the origin of this discrepancy, as the dimensions from a 2D plane have been taken into account, [55]. In addition to that and as blending of polymers might generate additional free volume as discussed before, it can affect the simulated value [45]. The increase in the free volume can decrease the density of the PEI nodules generating a decrease in the relative permittivity value and thus can affect the simulated value. From the TEM image in Fig. 3, an interphase exists between the PEI nodule and the epoxy system. This interphase can be remaining low molar masses epoxy-amine dissolved in the PEI phase and can also contain free volume as discussed previously. The presence of epoxy-diamine dissolved in a PEI phase can form a system that have different permittivity value except that it cannot affect the relative permittivity value of the blend as this interphase have relatively small percentage in comparison with the present PEI nodules and it is not present on all the nodules. Free volume that might be present in the PEI nodules will make a system which have lower density and thus can change the effect of PEI nodules on the mixture's the permittivity value.

Moreover, And finally, as the effective permittivity is not only affected by the fraction volume and the permittivity of the different constituents, proper determination of the form of the particle–particle and particle– network interaction potentials is necessary for further computing [56]. There are several factors that can affect the relative permittivity value of an epoxy blend and thus additional studies can be further suggested in this domain.

4. Conclusion

In this paper, the effect of phase separation phenomenon in the epoxy/thermoplastic blend on the thermal, mechanical and electrical properties was examined. The phase separation phenomenon taking place between the epoxy network and PEI nodules was illustrated by SEM imaging and confirmed by having two different transition processes in the DM10PEI system by DSC and DMA measurements. TEM images explored the presence of an interphase that surrounds PEI nodules; this cannot explain the presence of the shift taking place in the value of α relaxation temperature corresponding to the PEI inclusions. This interphase might correspond to remaining low molar masses of epoxy-amine dissolved in the PEI phase. However, the presence of free volume in the PEI nodules,

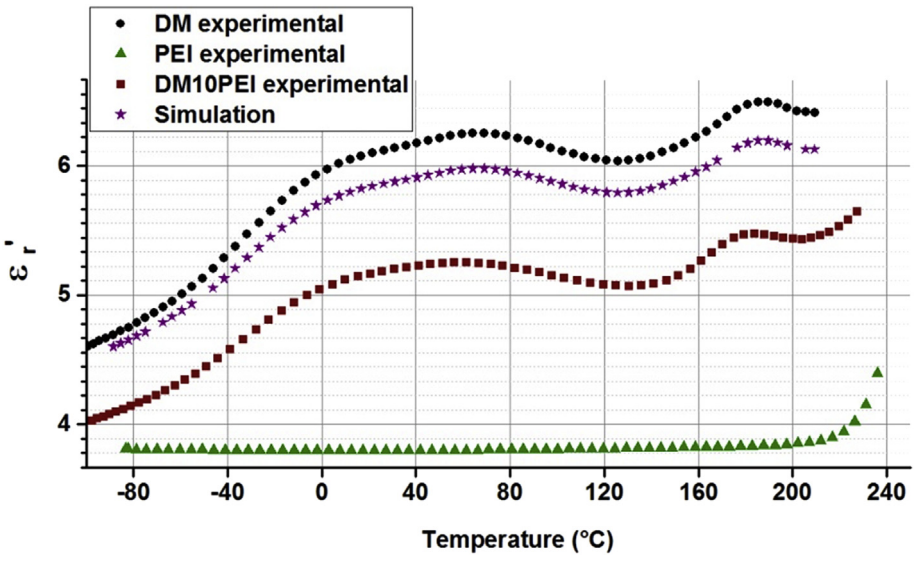

Fig. 10. Experimental permittivity at 1 kHz for DM, DM10PEI and PEI; effective simulated permittivity of DM10PEI.

which decreases the density of the material, can change the aspect of the PEI influencing the permittivity of the mixture. The addition of PEI into the epoxy system did not affect either the storage modulus or the thermal resistance under air or nitrogen atmosphere. Despite the fact, the real and imaginary parts of the relative permittivity of the whole system decreased by 15% in all the temperature and the frequency ranges. This decrease is also investigated by means of simulation and it is seen that a shift of 9% from the experimental values was observed which can be due to several phenomena as the existence of excluded volumes that can't be visualized via 2D SEM image, and the presence of free volumes from the fabrication process as discussed.

This novel proposed material with phase separation phenomenon is a good candidate for electrical insulation as the real and imaginary relative permittivity values have decreased in all temperature values up to 230 °C.

Acknowledgements

The authors wish to thank Pierre Alcouffe for realizing the TEM image at the Centre Technologique des Microstructures CTμ of the University of Lyon and the CLYM (Centre LYonnais des Microscopies) for giving us the access to use the ESEM. The French Ministry of Education and Research is gratefully recognized for providing a grant for this project and the Ecole Doctorale Electronique Electrotechnique Automatique de Lyon ED160 for their financial support.

References

[1] Tagare DM. Risks, operation, and maintenance of hydroelectric generators. Electric power generation. John Wiley & Sons, Inc; 2011. p. 15–43.
[2] Sichel EK, Gittleman JI, Sheng P. Electrical properties of carbon-polymer composites. JEM 1982;11:699–747. http://dx.doi.org/10.1007/BF02672392.
[3] Barber P, Balasubramanian S, Anguchamy Y, Gong S, Wibowo A, Gao H, et al. Polymer composite and nanocomposite dielectric materials for pulse power energy storage. Materials 2009;2:1697–733. http://dx.doi.org/10.3390/ma2041697.
[4] Phuchaduek W, Jamnongkan T, Rattanasak U, Boonsang S, Kaewpirom S. Improvement in physical and electrical properties of poly(vinyl alcohol) hydrogel conductive polymer composites. J Appl Polym Sci 2015;132. http://dx.doi.org/10.1002/app.42234. n/a-n/a.
[5] Van Velthem P, Ballout W, Horion J, Janssens Y-A, Destoop V, Pardoen T, et al. Morphology and fracture properties of toughened highly crosslinked epoxy composites: a comparative study between high and low Tg tougheners. Composites Part B:Engineering 2016;101:14–20. http://dx.doi.org/10.1016/j.compositesb.2016.06.076.
[6] Gupta AK, Harsha SP. Analysis of mechanical properties of carbon nanotube reinforced polymer composites using multi-scale finite element modeling approach. Compos Part B Eng 2016;95:172–8. http://dx.doi.org/10.1016/j.compositesb.2016.04.005.
[7] Zhao Y-H, Zhang Y-F, Bai S-L, Yuan X-W. Carbon fibre/graphene foam/polymer composites with enhanced mechanical and thermal properties. Compos Part B Eng 2016;94:102–8. http://dx.doi.org/10.1016/j.compositesb.2016.03.056.
[8] Lin J-H, Lin Z-I, Pan Y-J, Huang C-L, Chen C-K, Lou C-W. Polymer composites made of multi-walled carbon nanotubes and graphene nano-sheets: effects of sandwich structures on their electromagnetic interference shielding effectiveness. Compos Part B Eng 2016;89:424–31. http://dx.doi.org/10.1016/j.compositesb.2015.11.014.
[9] Tanaka T. Dielectric nanocomposites with insulating properties. IEEE Trans Dielectr Electr Insulation 2005;12:914–28. http://dx.doi.org/10.1109/TDEI.2005.1522186.
[10] Tsekmes IA, Morshuis PHF, Smit JJ, Kochetov R. Enhancing the thermal and electrical performance of epoxy microcomposites with the addition of nanofillers. IEEE Electr Insul Mag 2015;31:32–42. http://dx.doi.org/10.1109/MEI.2015.7089120.
[11] Iyer G, Gorur RS, Richert R, Krivda A, Schmidt LE. Dielectric properties of epoxy based nanocomposites for high voltage insulation. IEEE Trans Dielectr Electr Insulation 2011;18:659–66. http://dx.doi.org/10.1109/TDEI.2011.5931050.
[12] Castellon J, Nguyen HN, Agnel S, Toureille A, Frechette M, Savoie S, et al. Electrical properties analysis of micro and nano composite epoxy resin materials. IEEE Trans Dielectr Electr Insulation 2011;18:651–8. http://dx.doi.org/10.1109/TDEI.2011.5931049.
[13] Tsangaris GM, Kouloumbi N, Kyvelidis S. Interfacial relaxation phenomena in particulate composites of epoxy resin with copper or iron particles. Mater Chem Phys 1996;44:245–50. http://dx.doi.org/10.1016/0254-0584(96)80063-0.
[14] Tsekmes IA, Kochetov R, Morshuis PHF, Smit JJ. The role of particle distribution in the dielectric response of epoxy–boron nitride nanocomposites. J Mater Sci 2014;50:1175–86. http://dx.doi.org/10.1007/s10853-014-8674-5.
[15] Katayama J, Ohki Y, Fuse N, Kozako M, Tanaka T. Effects of nanofiller materials on the dielectric properties of epoxy nanocomposites. IEEE Trans Dielectr Electr Insulation 2013;20:157–65. http://dx.doi.org/10.1109/TDEI.2013.6451354.
[16] Tuncer E, Sauers I, James DR, Ellis AR, Paranthaman MP, Aytuğ T, et al. Electrical properties of epoxy resin based nano-composites. Nanotechnology 2007;18:25703. http://dx.doi.org/10.1088/0957-4484/18/2/025703.
[17] Han Z, Wood JW, Herman H, Zhang C, Stevens GC. Thermal properties of composites filled with different fillers. In: Conference record of the 2008 IEEE international symposium on electrical insulation. ISEI; 2008. p. 497–501. http://dx.doi.org/10.1109/ELINSL.2008.4570381. 2008, 2008.
[18] Heid T, Frechette M, David E. Nanostructured epoxy/POSS composites: high performance dielectrics with improved corona resistance and thermal conductivity. IEEE; 2014. p. 316–9. http://dx.doi.org/10.1109/EIC.2014.6869400.
[19] Preetha P, Thomas MJ. AC breakdown characteristics of epoxy nanocomposites. IEEE Trans Dielectr Electr Insulation 2011;(18):1526–34. http://dx.doi.org/10.1109/TDEI.2011.6032821.
[20] Maiez-Tribut S, Pascault JP, Soulé ER, Borrajo J, Williams RJJ. Nanostructured epoxies based on the self-assembly of block Copolymers: a new miscible block that can Be tailored to different epoxy formulations. Macromolecules 2007;40:1268–73. http://dx.doi.org/10.1021/ma062185l.
[21] Ritzenthaler S, Court F, Girard-Reydet E, Leibler L, Pascault JP. ABC triblock copolymers/epoxy-diamine blends. 2. Parameters controlling the morphologies and properties. Macromolecules 2003;36:118–26. http://dx.doi.org/10.1021/ma0211075.
[22] Rebizant V, Venet A-S, Tournilhac F, Girard-Reydet E, Navarro C, Pascault J-P, et al. Chemistry and mechanical properties of epoxy-based thermosets reinforced by reactive and nonreactive SBMX block copolymers. Macromolecules 2004;37:8017–27. http://dx.doi.org/10.1021/ma0490754.
[23] Girard-Reydet E, Vicard V, Pascault JP, Sautereau H. Polyetherimide-modified epoxy networks: influence of cure conditions on morphology and mechanical properties. J Appl Polym Sci 1997;65:2433–45. http://dx.doi.org/10.1002/(SICI)1097-4628(19970919)65. 12<2433::AID-APP15>3.0.CO;2–1.
[24] Williams RJJ, Rozenberg BA, Pascault J-P. Reaction-induced phase separation in modified thermosetting polymers. Polymer Analysis Polymer Physics. Springer Berl Heidelb 1997:95–156.
[25] Pascault JP, Williams RJJ. Formulation and characterization of thermoset/thermoplastic blends. In: Paul DR, Bucknall CB, editors. Polymer blends: formulation and performance. Wiley; 2000. p. 379–415 [Chapter 13].
[26] Hedrick JL, Yilgör I, Wilkes GL, McGrath JE. Chemical modification of matrix Resin networks with engineering thermoplastics. Polym Bull 1985;13:201–8. http://dx.doi.org/10.1007/BF00254652.
[27] Oyanguren PA, Riccardi CC, Williams RJJ, Mondragon I. Phase separation induced by a chain polymerization: polysulfone-modified epoxy/anhydride systems. J Polym Sci B Polym Phys 1998;36:1349–59. http://dx.doi.org/10.1002/(SICI)1099-0488(199806)36. 8<1349::AID-POLB9>3.0.CO;2-M.
[28] Yang G, Zheng B, Yang J-P, Xu G-S, Fu S-Y. Preparation and cryogenic mechanical properties of epoxy resins modified by poly(ethersulfone). J Polym Sci A Polym Chem 2008;46:612–24. http://dx.doi.org/10.1002/pola.22409.
[29] Blanco I, Cicala G, Faro CL, Recca A. Development of a toughened DGEBS/DDS system toward improved thermal and mechanical properties by the addition of a tetrafunctional epoxy resin and a novel thermoplastic. J Appl Polym Sci 2003;89:268–73. http://dx.doi.org/10.1002/app.12179.
[30] Hedrick JL, Yilgor I, Jurek M, Hedrick JC, Wilkes GL, McGrath JE. Chemical modification of matrix resin networks with engineering thermoplastics: 1. Synthesis, morphology, physical behaviour and toughening mechanisms of poly(arylene ether sulphone) modified epoxy networks. Polymer 1991;32:2020–32. http://dx.doi.org/10.1016/0032-3861(91)90168-I.
[31] Bucknall CB, Gilbert AH. Toughening tetrafunctional epoxy resins using polyetherimide. Polymer 1989;30:213–7. http://dx.doi.org/10.1016/0032-3861(89)90107-9.
[32] Girard-Reydet E, Sautereau H, Pascault JP, Keates P, Navard P, Thollet G, et al. Reaction-induced phase separation mechanisms in modified thermosets. Polymer 1998;39:2269–79. http://dx.doi.org/10.1016/S0032-3861(97)00425-4.
[33] Cho JB, Hwang JW, Cho K, An JH, Park CE. Effects of morphology on toughening of tetrafunctional epoxy resins with poly(ether imide). Polymer 1993;34:4832–6. http://dx.doi.org/10.1016/0032-3861(93)90005-U.
[34] Hourston DJ, Lane JM. The toughening of epoxy resins with thermoplastics: 1. Trifunctional epoxy resin-polyetherimide blends. Polymer 1992;33:1379–83. http://dx.doi.org/10.1016/0032-3861(92)90110-I.
[35] Bonnet A, Pascault JP, Sautereau H, Taha M, Camberlin Y. Epoxy–Diamine thermoset/thermoplastic blends. 1. Rates of reactions before and after phase separation. Macromolecules 1999;32:8517–23. http://dx.doi.org/10.1021/ma981754p.
[36] Riccardi CC, Borrajo J, Williams RJJ, Girard-Reydet E, Sautereau H, Pascault JP. Thermodynamic analysis of the phase separation in polyetherimide-modified epoxies. J Polym Sci B Polym Phys 1996;34:349–56. http://dx.doi.org/10.1002/(SICI)1099-0488(19960130)34. 2<349::AID-POLB16>3.0.CO;2-J.

[37] Gilbert AH, Bucknall CB. Epoxy resin toughened with thermoplastic. Makromol Chem Macromol Symp 1991;45:289–98. http://dx.doi.org/10.1002/masy.19910450129.
[38] Bonnet A, Lestriez B, Pascault JP, Sautereau H. Intractable high-Tg thermoplastics processed with epoxy resin: interfacial adhesion and mechanical properties of the cured blends. J Polym Sci B Polym Phys 2001;39:363–73. http://dx.doi.org/10.1002/1099-0488(20010201)39. 3<363::AID-POLB1008>3.0.CO;2-Q.
[39] Girard-Reydet E, Riccardi CC, Sautereau H, Pascault JP. Epoxy-aromatic diamine kinetics. Part 1. Modeling and influence of the diamine structure. Macromolecules 1995;28:7599–607. http://dx.doi.org/10.1021/ma00127a003.
[40] Bucknall CB, Yoshii T. Relationship between structure and mechanical properties in rubber-toughened epoxy resins. Brit Poly J 1978;10:53–9. http://dx.doi.org/10.1002/pi.4980100110.
[41] MacKinnon AJ, Jenkins SD, McGrail PT, Pethrick RA. A dielectric, mechanical, rheological and electron microscopy study of cure and properties of a thermoplastic-modified epoxy resin. Macromolecules 1992;25:3492–9. http://dx.doi.org/10.1021/ma00039a029.
[42] Levchik SV, Weil ED. Thermal decomposition, combustion and flame-retardancy of epoxy resins—a review of the recent literature. Polym Int 2004;53:1901–29. http://dx.doi.org/10.1002/pi.1473.
[43] Heux L, Halary JL, Lauprêtre F, Monnerie L. Dynamic mechanical and 13C n.m.r. investigations of molecular motions involved in the β relaxation of epoxy networks based on DGEBA and aliphatic amines. Polymer 1997;38:1767–78. http://dx.doi.org/10.1016/S0032-3861(96)00694-5.
[44] Wan J, Li C, Bu Z-Y, Xu C-J, Li B-G, Fan H. A comparative study of epoxy resin cured with a linear diamine and a branched polyamine. Chem Eng J 2012;188:160–72. http://dx.doi.org/10.1016/j.cej.2012.01.134.
[45] Akay M, Cracknell JG. Epoxy resin–polyethersulphone blends. J Appl Polym Sci 1994;52:663–88. http://dx.doi.org/10.1002/app.1994.070520509.
[46] Choudhury A. Dielectric and piezoelectric properties of polyetherimide/BaTiO3 nanocomposites. Mater Chem Phys 2010;121:280–5. http://dx.doi.org/10.1016/j.matchemphys.2010.01.035.
[47] Heid T, Fréchette M, David E. Epoxy/BN micro- and submicro-composites: dielectric and thermal properties of enhanced materials for high voltage insulation systems. IEEE Trans Dielectr Electr Insulation 2015;22:1176–85. http://dx.doi.org/10.1109/TDEI.2015.7076820.
[48] Nelson JK, Fothergill JC. Internal charge behaviour of nanocomposites. Nanotechnology 2004;15:586. http://dx.doi.org/10.1088/0957-4484/15/5/032.
[49] Singha S, Thomas MJ. Dielectric properties of epoxy nanocomposites. IEEE Trans Dielectr Electr Insulation 2008;15:12–23. http://dx.doi.org/10.1109/T-DEI.2008.4446732.
[50] Fothergill JC, Nelson JK, Fu M. Dielectric properties of epoxy nanocomposites containing TiO2, Al2O3 and ZnO fillers. In: 2004 annual report conference on electrical insulation and dielectric phenomena. CEIDP '04; 2004. p. 406–9. http://dx.doi.org/10.1109/CEIDP.2004.1364273. 2004.
[51] Polder D, van Santeen JH. The effective permeability of mixtures of solids. Physica 1946;12:257–71. http://dx.doi.org/10.1016/S0031-8914(46)80066-1.
[52] Fricke H. The maxwell-wagner dispersion in a suspension of ellipsoids. J Phys Chem 1953;57:934–7. http://dx.doi.org/10.1021/j150510a018.
[53] Altshuller AP. The shapes of particles from dielectric constant studies of suspensions. J Phys Chem 1954;58:544–7. http://dx.doi.org/10.1021/j150517a008.
[54] Asami K. Characterization of heterogeneous systems by dielectric spectroscopy. Prog Polym Sci 2002;27:1617–59. http://dx.doi.org/10.1016/S0079-6700(02)00015-1.
[55] Balberg I, Anderson CH, Alexander S, Wagner N. Excluded volume and its relation to the onset of percolation. Phys Rev B 1984;30:3933–43. http://dx.doi.org/10.1103/PhysRevB.30.3933.
[56] Brosseau C. Modelling and simulation of dielectric heterostructures: a physical survey from an historical perspective. J Phys D Appl Phys 2006;39:1277. http://dx.doi.org/10.1088/0022-3727/39/7/S02.